

On the gravitational content of molecular clouds and their cores

Javier Ballesteros-Paredes¹ *, Gilberto C. Gómez¹, Bárbara Pichardo², and Enrique Vázquez-Semadeni¹

¹ *Centro de Radioastronomía y Astrofísica, Universidad Nacional Autónoma de México, Apdo. Postal 72-3 (Xangari), Morelia, Michocán 58089, México*

² *Instituto de Astronomía, Universidad Nacional Autónoma de México, Apdo. Postal 70-264, 04510, México, D.F., México*

Submitted to MNRAS, 30 October 2018

ABSTRACT

The gravitational term for clouds and cores entering in the virial theorem is usually assumed to be equal to the gravitational energy, since the contribution to the gravitational force from the mass distribution outside the volume of integration is assumed to be negligible. Such approximation may not be valid in the presence of an important external net potential. In the present work we analyze the effect of an external gravitational field on the gravitational budget of a density structure. Our cases under analysis are (a) a giant molecular cloud (GMC) with different aspect ratios embedded within a galactic net potential, including the effects of gravity, shear, and inertial forces, and (b) a molecular cloud core embedded within the gravitational potential of its parent molecular cloud.

We find that for roundish GMCs, the tidal tearing due to the shear in the plane of the galaxy is compensated by the tidal compression in the z direction. The influence of the external effective potential on the total gravitational budget of these clouds is relatively small (up to $\sim 15 - 25\%$), although not necessarily negligible. However, for more filamentary GMCs, elongated on the plane of the galaxy, the external effective potential can be dominant and can even overwhelm self-gravity, regardless of whether its main effect on the cloud is to disrupt it or compress it. This may explain the presence of some GMCs with few or no signs of massive star formation, such as the Taurus or the Maddalena's clouds.

In the case of dense cores embedded in their parent molecular cloud, we found that the gravitational content due to the external field may be more important than the gravitational energy of the cores themselves. This effect works in the same direction as the gravitational energy, i.e., favoring the collapse of cores. We speculate on the implications of these results for star formation models, in particular that apparently nearly magnetically critical cores may actually be supercritical due to the effect of the external potential.

Key words: Galaxies: kinematics and dynamics – ISM: general – clouds – kinematics and dynamics – Stars: formation

1 INTRODUCTION

All known star formation in the Galaxy occurs within dense cores in molecular clouds (MCs). The detailed physical nature of such molecular clouds and their dense cores has been a matter of debate over the years. In particular, the su-

personic linewidths of CO observed in molecular clouds for first time by Wilson et al. (1970) was suggested as indicative of gravitational contraction by Goldreich & Kwan (1974). However, Zuckerman & Evans (1974) subsequently argued that, if MCs were collapsing, the star formation efficiency should be much larger than observed, and that the molecular gas in our galaxy should already be exhausted. These authors suggested, instead, that the supersonic linewidths

* e-mail: j.ballesteros@crya.unam.mx

were evidence of supersonic turbulence. This idea was widely accepted, and turbulence was assumed to be a key ingredient of molecular cloud support against self-gravity. For instance, de Jong et al. (1980) calculated hydrostatic models of molecular clouds supported by turbulent (ram) pressure, while Larson (1981) found two scaling relations for atomic and molecular clouds which were compatible with them being gravitationally bound and in approximate virial equilibrium. Since then, many observational studies claim that molecular clouds and their cores are close to energy equipartition (most often referred to as “virial equilibrium”, although this is not necessarily so; see Ballesteros-Paredes 2006) between self-gravity, kinetic energy, and, when the measurements were available, the magnetic energy (e.g., Myers & Goodman 1988a,b; Heiles & Troland 2005). While some authors supported the idea that MCs and their cores are self-gravitating (e.g., McKee and Zweibel 1992, although with some exceptions, see Bertoldi & McKee (1992)), others argued that MCs may not be self-gravitating (Blitz 1994), and will “need” an external pressure, in order to be confined (e.g., Maloney 1988).

With the development of numerical simulations in the last decade, it became clear that molecular clouds and their cores can exhibit Larson (1981)-type relationships (Vázquez-Semadeni et al. 1997; Ballesteros-Paredes & Mac Low 2002), and near energy equipartition (Ballesteros-Paredes & Vázquez-Semadeni 1995), but they are not in virial *equilibrium* (Ballesteros-Paredes & Vázquez-Semadeni 1997; Shadmehri et al. 2002; Tilley & Pudritz 2004; Ballesteros-Paredes 2006; Dib et al. 2007). Such clouds and their cores can be also more transient¹ than previously thought, a fact that is compatible with the lack of post-T Tauri stars (~ 10 Myr old stars) associated to molecular clouds (Briceño et al. 1997; Ballesteros-Paredes et al. 1999; Hartmann et al. 2001; Ballesteros-Paredes & Hartmann 2007).

In most virial balance analyses of molecular clouds and dense cores, one of the key assumptions is often that the gravitational term entering the virial theorem for a cloud or core is given only by its gravitational energy,

$$E_{\text{grav}} = \frac{1}{2} \int_V \rho \Phi dV, \quad (1)$$

where Φ is the gravitational potential produced by the density ρ in the volume V , thus neglecting the gravitational field due to the mass distribution outside the volume V . However, in principle the mass external to the volume of integration can also influence the energy budget of the cloud/core (Spitzer 1978; Ballesteros-Paredes 2006). The external distribution of mass, together with external forces (such as centrifugal and Coriolis forces) may either tend to tear apart or to compress the cloud/core under analysis.

The goal of the present work is to numerically evaluate how realistic is the third Virial Theorem “Myth” discussed by Ballesteros-Paredes (2006), namely, that the gravitational term can be approximated by the gravitational

energy. We aim to compare the gravitational energy with the effect of external forces for the cases of giant molecular clouds (GMCs), as well as of the dense cores within them. Thus, we evaluate the full external potential term in the virial theorem for both (i) a typical GMC within the Galaxy, and (ii) a typical dense core within the gravitational potential of its parent molecular cloud.

The organization of the paper is as follows. In §2 we provide a physical interpretation for the external gravitational term W_{ext} , and its contribution to the energy budget of a volume of interest. In §3 we discuss the cases under analysis, and in §4 we present our results. Finally, in §5 we summarize our results, and discuss their physical implications, emphasizing their consequences on models of star formation.

2 TIDAL ENERGY ENTERING THE VT

The gravitational term entering the VT, given by

$$W \equiv - \int_V x_i \rho \frac{\partial \Phi}{\partial x_i} dV, \quad (2)$$

is usually taken to be equal to the gravitational energy of the cloud, i.e.,

$$W \simeq E_{\text{grav}} \equiv 1/2 \int_V \rho \Phi_{\text{cloud}} dV, \quad (3)$$

where ρ is the density, Φ is the total gravitational potential, and

$$\Phi_{\text{cloud}} = -G \int_V \frac{\rho(\mathbf{x}')}{|\mathbf{x} - \mathbf{x}'|} dV \quad (4)$$

is the gravitational potential of the cloud, i.e., due only to the mass distribution inside the volume V of the cloud. This approximation is valid only if the cloud is isolated, i.e., if the forces from external agents are negligible compared to the self-gravity of the cloud (e.g., Chandrasekhar & Fermi 1953). However, MCs in disk galaxies are confined to the midplane ($z \sim \pm 50$ pc). Within these disks, most of the mass in molecular gas is well organized into spiral arms, bars and/or rings (e.g., Young & Scoville 1991; Downes et al. 1996; Loinard et al. 1996, 1999; Dame et al. 2001; Helfer et al. 2003), following the gravitational potential of the old stars, which dominates the dynamics (Binney & Tremaine 1987). These patterns suggest, thus, that the Galactic gravitational field may be playing a crucial role in the global gravitational budget of MCs. An important issue is thus to determine the effect of tidal forces on the clouds and their effect on preventing or inducing their collapse.

In order to calculate the contribution of the external potential to the energy budget of the cloud, let us separate the total gravitational potential into its component due to the mass of the cloud alone plus all external agents:

$$\Phi = \Phi_{\text{cloud}} + \Phi_{\text{ext}}, \quad (5)$$

where Φ_{ext} is the potential produced by all the mass outside the volume of the cloud. Thus, the gravitational term entering the VT can be written as:

$$W = E_{\text{grav}} + W_{\text{ext}} \quad (6)$$

where W_{ext} is given by

¹ By transient we mean clouds that either re-disperse into their environment, or collapse to form stars, but that in either case do not last much longer than their free-fall times.

$$W_{\text{ext}} \equiv - \int_V x_i \rho \frac{\partial \Phi_{\text{ext}}}{\partial x_i} dV. \quad (7)$$

This term represents the contribution to a cloud's gravitational budget from tidal forces. Note that we have defined W_{ext} with a minus sign, such that, if it is negative, it contributes to the collapse, just as the gravitational energy, but if it is positive, it acts against the gravitational energy by contributing to the disruption of the cloud. Furthermore, its sign is given by the mean concavity of the gravitational potential Φ_{ext} , being positive if the concavity faces downwards, and negative if it faces upwards. To visualize this, in Fig. 1 we draw schematically four different situations in which a spherical cloud is embedded in an external gravitational potential Φ_{ext} . In the first case, (top-left panel) the forces ($F = -\nabla\Phi_{\text{ext}}$) on the right-hand side of the cloud are stronger than the forces on the left-hand side. This is schematically represented by a darker and larger arrow on the right-hand side of the cloud, and with a larger absolute value of the slope of the external gravitational potential. Since the slope of Φ_{ext} is negative, the forces are positive, but stronger at the right- than at the left-side of the cloud. The net effect of such an external field is towards disrupting the cloud. In fact, for the left-hand side of the cloud, $x_i < 0$, $\partial\Phi_{\text{ext}}/\partial x_i < 0$. The product of these quantities is positive, and the minus sign of W_{ext} (eq. 7) gives a negative result for W_{ext} . However, for the right-hand side of the cloud, $x_i > 0$, and $\partial\Phi_{\text{ext}}/\partial x_i < 0$. The product is negative, and the minus sign in the definition of W_{ext} gives a positive value for W_{ext} . Given the symmetry of the cloud, and since the forces are larger on the right-hand side, the total value of W_{ext} is positive, i.e., the external field acts against the gravitational energy. In other words, the cloud is being torn apart by the external gravitational field.

For the second case (top-right panel), the dominant contribution is that from the left-hand side, and the cloud suffers a net external compression. In this case, a similar analysis gives $W_{\text{ext}} < 0$. Cases 3 and 4 (respectively, bottom left and right panels) can be analyzed in a similar way, and W_{ext} is negative and positive, respectively. In summary, W_{ext} contains the net effect of the tidal forces over the whole volume of the cloud, and its sign is defined by the curvature of the gravitational potential field.

Before ending the present section, it is useful to define

$$\begin{aligned} W_{\text{ext},x} &\equiv - \int_V x \rho \partial\Phi_{\text{ext}}/\partial x dV, \\ W_{\text{ext},y} &\equiv - \int_V y \rho \partial\Phi_{\text{ext}}/\partial y dV, \\ W_{\text{ext},z} &\equiv - \int_V z \rho \partial\Phi_{\text{ext}}/\partial z dV, \end{aligned} \quad (8)$$

such that $W_{\text{ext}} = W_{\text{ext},x} + W_{\text{ext},y} + W_{\text{ext},z}$, in order to understand how the three-dimensional potential works in each direction.

3 MODELING THE GRAVITATIONAL FIELD AND THE VOLUME OF INTEGRATION

We evaluate the virial gravitational term in two main cases: a giant molecular cloud (GMC) within a disk galaxy, and a molecular cloud core at different positions within its parent

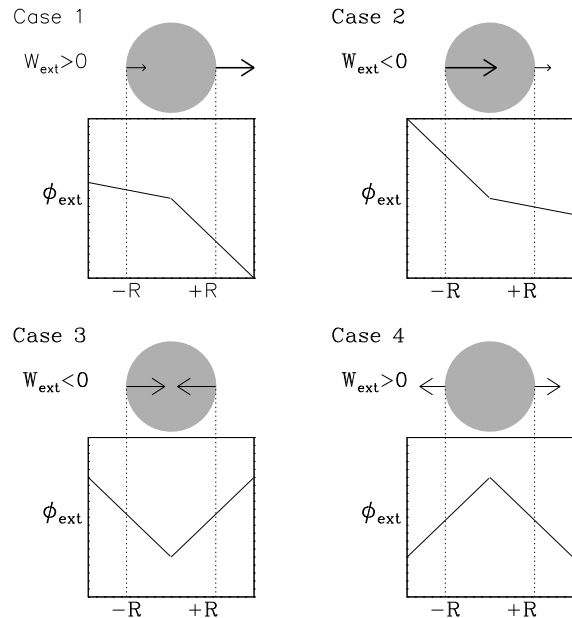


Figure 1. The tidal energy, W_{ext} , is positive if the concavity of the external potential Φ_{ext} faces downwards, and negative if it faces upwards.

molecular cloud. In every case, following eq. (5), we will assume that the total gravitational potential Φ is given by the addition of two independent potentials: that produced by the mass of the object under analysis (GMC or core, which will be called Φ_{cloud}), and the external potential (from the Galaxy or the GMC), which we will call Φ_{ext} .

3.1 Giant Molecular clouds within a disk galaxy

We first consider the effects of a galactic gravitational potential field over a giant molecular cloud. We consider a set of prolate clouds with constant density $n = 50 \text{ cm}^{-3}$, and major axis of 25 pc. The aspect ratios for each case are: 10:10 (spherical case), 10:8, 10:6, 10:4, 10:2, and 10:1. We align those spheroids in both the x - and y -directions, in order to see how the cloud's energy budget varies as a function of the relative orientation of the spheroids and the spiral arms within the galaxy.

The clouds are located within a spiral galaxy with a gravitational potential field given by the model implemented by Pichardo et al. (2003). This model uses an axisymmetric background potential that assembles a bulge, a flattened disk with a scale-height of 250 pc, as proposed by Miyamoto & Nagai (1975), and a massive halo extending to a radius of 100 kpc, as proposed by Allen & Santillán (1991). The main adopted parameters are $R_0 = 8.5 \text{ kpc}$ as the Sun's galactocentric distance, and $V_0(R_0) = 220 \text{ km s}^{-1}$ as the circular velocity at the Sun's position. The total mass is $9 \times 10^{11} M_{\odot}$, and the local escape velocity is 536 km s^{-1} . The local total mass density is $\rho_0 = 0.15 M_{\odot} \text{ pc}^{-3}$. The resulting values for Oort's constants are $A = 12.95 \text{ km s}^{-1} \text{ kpc}^{-1}$ and $B = -12.93 \text{ km s}^{-1} \text{ kpc}^{-1}$. The full expressions of the axisymmetric potential can be found in Allen & Santillán (1991).

In addition to the axisymmetric potential, we have im-

plemented a bi-symmetric spiral model constructed with oblate spheroids as those proposed by Schmidt (1956) using the spiral logarithmic locus proposed by Roberts et al. (1979). The parameters for the spiral arms based on self-consistency studies and a compilation of observational results (Pichardo et al. 2003) are: the pitch angle is $i_p = 15.5^\circ$; the galactocentric radii at which the arms start and end are, respectively $r_s = 3.3$ kpc and $r_e = 12$ kpc; the width of the spiral arms is 2 kpc. The density fall along the spiral arm is exponential with the same scale-length as the disk (2.5 kpc). Finally, the ratio of spiral mass to disk mass is $M_S/M_D = 0.0175$, which represents a lower limit on the range given by self-consistency analysis.

Every point in the volume of integration will be analyzed in a frame of reference located at the center of the cloud, which rotates around the Galactic center. This adds a centrifugal potential that produces the force

$$F_{\text{centrif}} = -\frac{\partial\Phi_{\text{centrif}}}{\partial r} = \Omega_0^2 r \hat{e}_r, \quad (9)$$

where Ω_0 is the angular velocity of the reference frame that rotates with the center of the cloud, r is the galactocentric distance of the fluid element under consideration, and \hat{e}_r is the unit vector in the direction of the galactocentric radius. It is also necessary to account for the Coriolis term in our modified potential:

$$F_{\text{cor}} = -\frac{\partial\Phi_{\text{cor}}}{\partial r} = 2\Omega_0 v \hat{e}_r, \quad (10)$$

where v is the velocity of the point in the volume of integration, measured in the frame of reference of the center of the cloud, i.e., in the frame that moves with angular frequency Ω_0 . With this in mind, the effective potential entering in eqs. (6) and (7) is given by

$$\begin{aligned} \nabla\Phi_{\text{eff}} &= \nabla\Phi_{\text{gal}} + \nabla\Phi_{\text{centrif}} + \nabla\Phi_{\text{cor}} \\ &= \nabla\Phi_{\text{gal}} - (\Omega_0^2 r + 2\Omega_0 v) \hat{e}_r. \end{aligned} \quad (11)$$

Note that this potential assumes perfect circular orbits, while actual orbits are not necessarily perfect circles. However, the velocities in both cases are similar within a factor not larger than 10%. Since the velocities entering in eq. (11) affect two of the three terms, we do not expect changes larger than 10%.

3.2 Dense cores within a molecular cloud

In addition to the molecular cloud embedded within a spiral galaxy, we analyze the gravitational budget of smaller structures: dense cores embedded within its parent GMC. Although molecular clouds and their cores exhibit substantial substructure over a wide range of sizes (e.g., Falgarone et al. 1991), we will consider, for simplicity, that our test core is spherical, with constant density ($n = 3500 \text{ cm}^{-3}$), and size $R_{\text{core}} = 0.5$ pc, which are typical of dense dark cloud cores (Troland & Crutcher 2008). We also model the gravitational potential field of the parent molecular cloud with a Plummer (1911) potential, as used by Gieles et al. (2006), who analyzed the evolution of a stellar cluster interacting with a giant molecular cloud. Such potential is written as

$$\Phi_{\text{ext}} = -\frac{GM_{\text{GMC}}}{\sqrt{r^2 + a^2}}, \quad (12)$$

with $a = r_{\text{GMC}}/2$. Following Gieles et al. (2006), we relate the mass and size of the GMC by a Larson (1981) type relation².

$$M_{\text{GMC}} = 540M_{\odot} \left(\frac{r_{\text{GMC}}}{1 \text{ pc}} \right)^2, \quad (13)$$

which, for $M_{\text{GMC}} = 10^4 M_{\odot}$ yields $r_{\text{GMC}} = 4.30$ pc. For these parameters, the GMC's central density is $4.13 \times 10^3 \text{ cm}^{-3}$.

Since GMCs frequently exhibit elongated or filamentary structure, we consider two other simple cases of modified Plummer spheres (a detailed analysis including a variety of more realistic parent cloud structures will be presented in a future contribution). In the first place, we studied the superposition of two Plummer spheroids: one centered at $x = 0$ and with mass M_{GMC} , and the second centered at $x = 3r_{\text{GMC}}$, with a mass $4M_{\text{GMC}}$, and a radius twice as large, according to eq. (13).

Finally, we modify the Plummer (1911) potential to obtain an elongated structure, in order to mimic a filamentary cloud. In this case, the external potential is given by

$$\Phi_{\text{ext}} = -\frac{GM_{\text{GMC}}}{\sqrt{\tilde{r}^2 + a^2}}, \quad (14)$$

where

$$\frac{\tilde{r}(x, y, z)}{r_{\text{GMC}}} = \left[\left(\frac{x}{r_x} \right)^2 + \left(\frac{y}{r_y} \right)^2 + \left(\frac{z}{r_z} \right)^2 \right]^{1/2}, \quad (15)$$

$r_x = r_{\text{GMC}} f^{2/3}$ and $r_y = r_z = r_{\text{GMC}} f^{-1/3}$, where f is the aspect ratio of the resulting spheroid. For $f = 10$, $r_x = 20$ pc and $r_y = r_z = 2$ pc. The parameters M_{GMC} and r_{GMC} are related also by eq. (13).

4 RESULTS

4.1 The molecular cloud within a disk galaxy

Figures 2 and 3 show the ratios $W_{\text{ext}}/E_{\text{grav}}$ through the galaxy at $z = 0$ for our prolate spheroidal GMCs ($n = 50 \text{ cm}^{-3}$, long axis $R_{\text{cloud}} = 25$ pc on the plane of the galaxy, and aspect ratios of 10:10, 10:8, 10:6, 10:4, 10:2 and 10:1, along the x - and y -directions, respectively).

The first important result is that the term due to the external potential, W_{ext} , does not seem to be negligible in most of places within the galaxy. This is in clear contrast with the typical assumptions in the literature, where the gravitational energy E_{grav} is thought to be the quantity to be compared to other kind of energies in order to explain collapse, support, or expansion. Secondly, the maximum and minimum possible values of the ratio $W_{\text{ext}}/E_{\text{grav}}$ are quite similar for both (x - and y - alignment) cases, although the structure of the images differs substantially, specially in the cases with large aspect ratios (panels d,e,f in both figures).

² Note that this relation has been highly questioned, since it seems to be more a consequence of observational biases, rather than a true relationship (Kegel 1989; Scalo 1990; Vázquez-Semadeni et al. 1997; Ballesteros-Paredes & Mac Low 2002). However, for the sake of simplicity, the models of clouds that we analyzed follow this relationship.

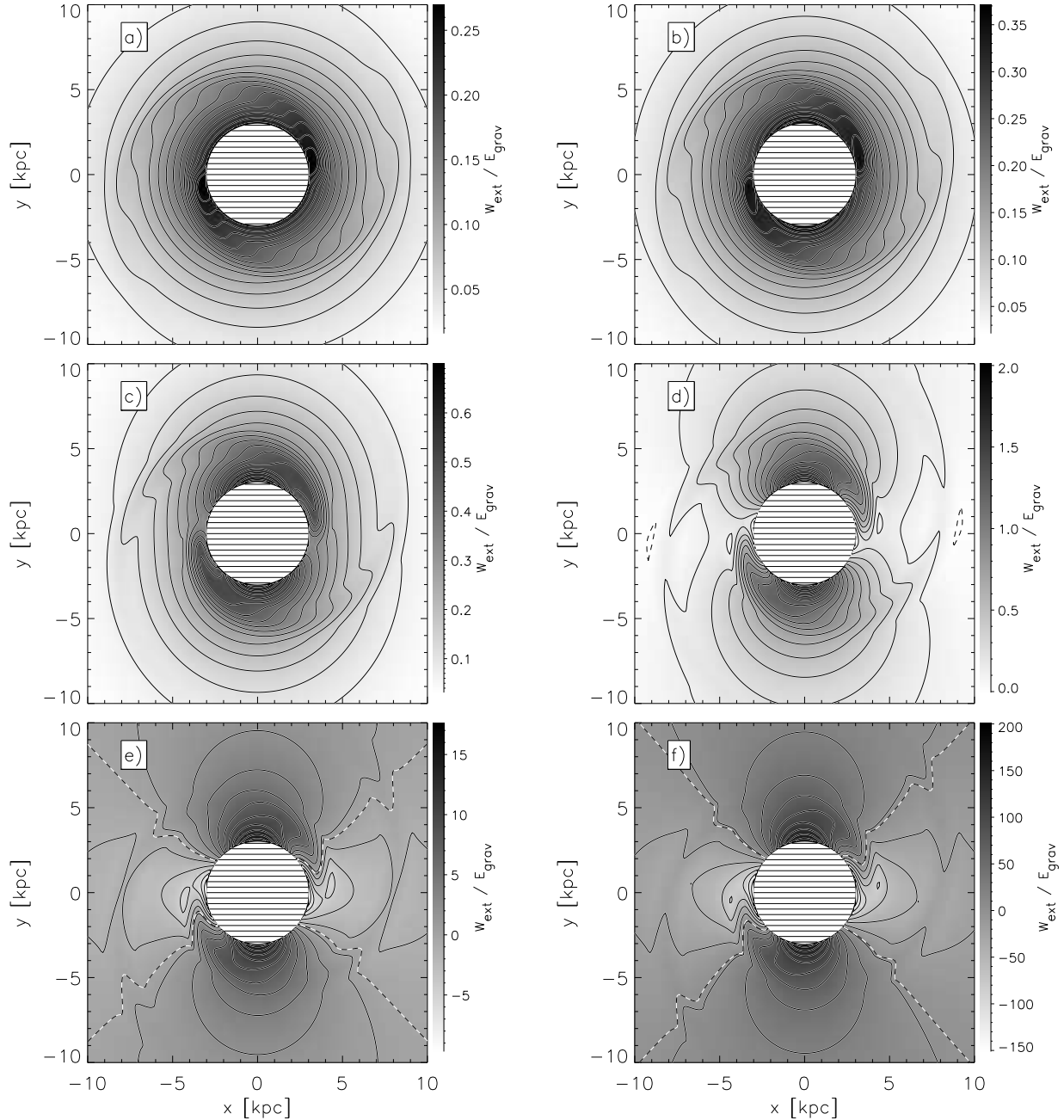


Figure 2. Grayscale map of the ratio $W_{\text{ext}}/E_{\text{grav}}$ for GMCs (represented as prolate spheroids) aligned with the x axis. A central circle ($r \leq 3$ kpc) is excluded from the calculation since there are some missing physical ingredients, such as a galactic bar potential. The dashed line represents the $W_{\text{ext}} = 0$ level. Each case is a prolate spheroid, with larger-to-smaller ratio of (a) 10:10, (b) 10:8, (c) 10:6, (d) 10:4, (e) 10:2 and (f) 10:1, respectively. Note that, for clouds with small axis larger than 10 pc (cases a, b, c, and d), the ratio is positive, i.e., W_{ext} acts in the same sense as gravity. This is due mainly to the strong curvature of the gravitational potential along the galactic height z , which dominates in compressing the cloud against any tidal disruption imposed by the shear and/or tidal streams from the spiral arms. However, for clouds elongated in the plane of the galaxy by a factor of $\sim 10:4$ or more (cases e and f), either tidal stretching or compression can dominate the energy budget, depending on the position and orientation of the filament in the galaxy. This result suggests that the intensity of star formation of a cloud may have a strong dependence on its morphology, its position and its orientation within the galaxy.

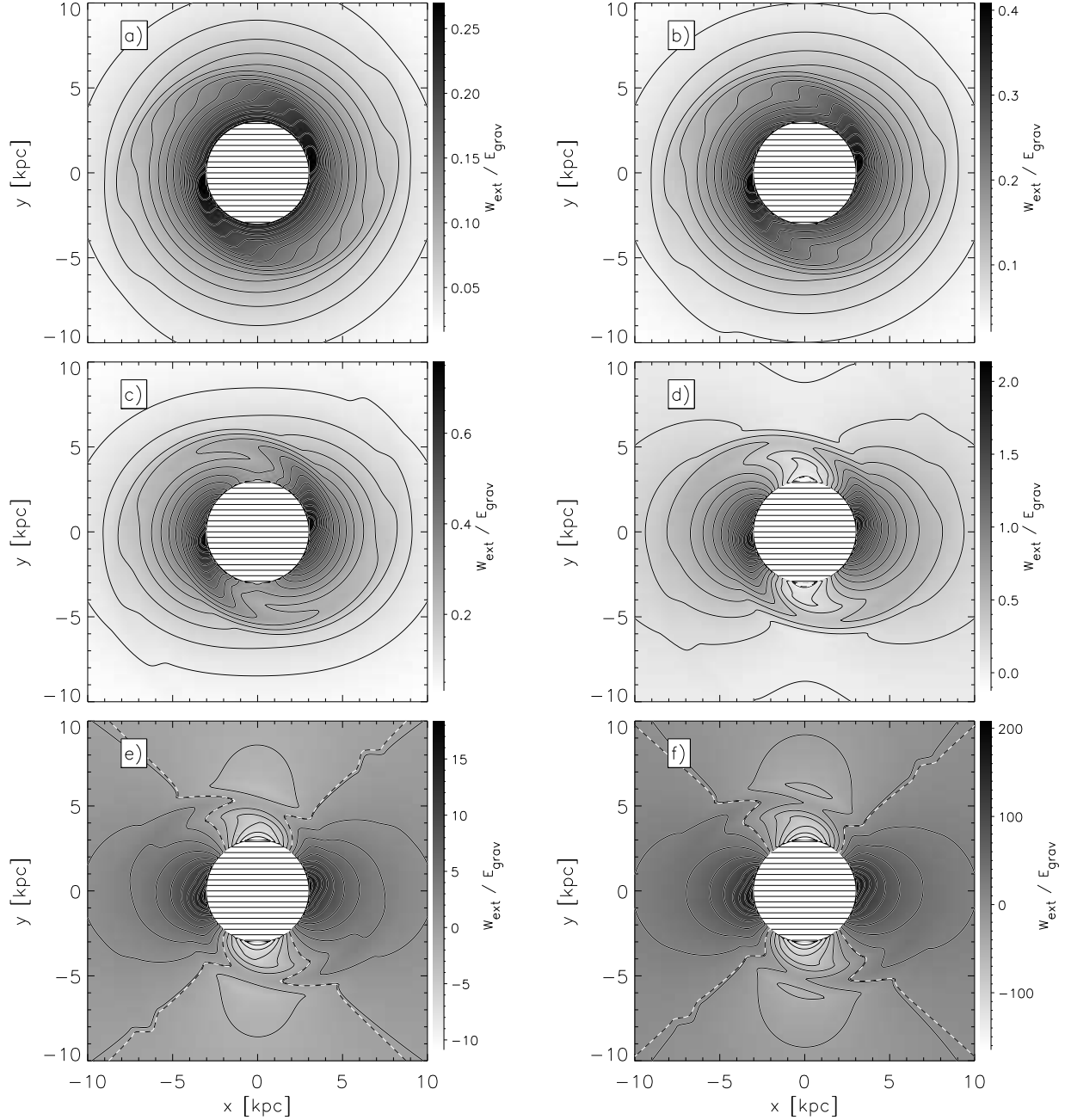


Figure 3. Same as Fig. 2, but for spheroids aligned with the y -axis.

We also note that, for the more roundish clouds (cases a, b, c, d), the effective potential of the galaxy works in the same direction as the self-gravity, giving positive values of the term $W_{\text{ext}}/E_{\text{grav}}$. This is so because, while the effective potential imposes a shear that tries to disrupt the clouds in the plane of the galaxy (i.e., $W_{\text{ext},x} + W_{\text{ext},y} > 0$), the gravitational potential of the galaxy along the z axis has a confining effect, and it may dominate if the cloud is long

enough along z compared to its dimensions on the plane of the galaxy. The situation is, however, somewhat different for more elongated clouds that do not extend very much in z (panels d, e, f). In these cases, the effective gravitational field of the rotating cloud may work either by compressing (darker zones) or disrupting (light zones) the cloud, depending on the region where the cloud is located within the galaxy. Furthermore, by comparing Figs. 2 and 3, it can

be noticed that if the filamentary cloud is perpendicular to the radius of the galaxy, the external field works toward compressing the cloud (darker zones), while if it is parallel to the radius of the galaxy, the external field tries to disrupt it (light zones), even if it is close to the spiral arms. This result is due to the differential rotation, since a cloud aligned with the radius of the galaxy will feel the galactic differential rotation much more strongly than a cloud that is perpendicular to it.

Finally, it is interesting to note that, for the roundish cases, the external contribution to the gravitational budget is not larger than $\sim 25\%$. However, for the more elongated cases, this contribution can be a large factor, suggesting that some filamentary GMCs may actually be gravitationally unbound. This could be the case, for instance, of those few GMCs that exhibit no signs of massive star formation, yet have masses of the order of 10^4 - $10^5 M_\odot$ (e.g., Taurus, G 216-2.5, Coalsack).

One may ask how much these results can vary with the parameters of the cloud (size and density). Let us assume that the cloud is “small enough”, so that the external forces over the cloud can be approximated by linear functions of the distance to the center of the cloud, then $\nabla\Phi_{\text{ext}} \propto R_{\text{cloud}}$. In this case, $W_{\text{ext}} \propto \rho R_{\text{cloud}}^5$, while $E_{\text{grav}} \propto M^2/R_{\text{cloud}} \propto \rho^2 R_{\text{cloud}}^5$. Then, the ratio $W_{\text{ext}}/E_{\text{grav}} \propto 1/\rho_{\text{cloud}}$. Thus, for a given shape of the cloud, the ratio $W_{\text{ext}}/E_{\text{grav}}$ can be scaled to different densities as $1/\rho_{\text{cloud}}$. In our case, “small enough” is smaller than ~ 50 pc.

In the present work, we have decided to keep the density constant and vary the shape of the clouds. However, it is possible in principle that the resulting increase of $W_{\text{ext}}/E_{\text{grav}}$ for spherical clouds for elongated clouds could be due to a decrease in the clouds’ mass, and therefore their gravitational energy as the shape becomes more elongated, giving the impression of an increase in the relative importance of W_{ext} . Therefore, another plausible scenario to explore would be to fix the mass, or the column density, while varying other parameters of the cloud. However, our results can be translated to those cases. For instance, since $W_{\text{ext}}/E_{\text{grav}} \propto 1/\rho_{\text{cloud}}$, by keeping constant the mass of the clouds, the ratio $W_{\text{ext}}/E_{\text{grav}}$ grows with size as R_{cloud}^3 . In the case of constant column density, the $W_{\text{ext}}/E_{\text{grav}} \propto R_{\text{cloud}}$. In order to show that this is the case, in Fig. 4 displays three panels with the ratio $W_{\text{ext}}/E_{\text{grav}}$ for spherical clouds as a function of $x \geq 0$ ($y = 0, z = 0$) for clouds with different densities but same size (left panel), different sizes but same mass (middle panel), and different sizes, but same column density (right panel). It can be seen that $W_{\text{ext}}/E_{\text{grav}} \propto 1/\rho$ for all cases (and then $\propto R^3$ and $\propto R$ for the constant mass and column density respectively). Thus, for a given cloud, one can calculate its mass, or its column density, and then, calculate how much the ratio $W_{\text{ext}}/E_{\text{grav}}$ will vary if the size varies too.

We finally note that our results do not change strongly by placing the clouds above or below the plane of the galaxy. At first glance, one might think that a cloud located 50 or 100 pc away from the midplane will experience a tidal stress along z , rather than a tidal compression. However, we note that the gravitational potential along z has always positive concavity, and then the situation is just like the one shown in Fig 1, cases 2 or 3. It is important to note, however, that the radius of curvature of the gravitational potential grows

with z , and thus the vertical compression decreases as z increases.

4.2 The core within a GMC

Figure 5 shows both the potential (upper panel) and the ratios $W_{\text{ext}}/E_{\text{grav}}$, $W_{\text{ext},x}/E_{\text{grav}}$, and $W_{\text{ext},y}/E_{\text{grav}}$ (lower panel) as a function of distance to the center of the cloud, for our dense core ($n = 3500 \text{ cm}^{-3}$, $R_{\text{core}} = 0.5$ pc) embedded in a single Plummer potential. As discussed in §2, the curvature of the potential defines whether W is positive or negative. For instance, $W_{\text{ext},x}$ is negative whenever Φ_{ext} has upwards concavity, and positive wherever Φ_{ext} has downward concavity. On the other hand, $W_{\text{ext},y}$ is always negative at every position along the x axis because, along the radius, Φ_{ext} has upwards concavity in the azimuthal direction.

More important, however, is to note in this figure that W_{ext} grows substantially when the core is located in the inner parts of the molecular cloud. In fact, it is larger (in absolute value) than E_{grav} at the central parts of the potential well, enhancing the importance of accounting for W_{ext} when analyzing the energy budget of dense cores.

As a step towards taking a more realistic potential for a molecular cloud, we show in Fig. 6 the potential (upper panel) and the ratios $W_{\text{ext}}/E_{\text{grav}}$, $W_{\text{ext},x}/E_{\text{grav}}$, and $W_{\text{ext},y}/E_{\text{grav}}$ (lower panel) for the same dense core embedded in the potential produced by two Plummer spheroids, centered at different locations ($x = y = z = 0$ pc), and $x = 12.5, y = z = 0$ pc), as a function of x . In Fig. 7 we show a grayscale $x - y$ map of the ratio $W_{\text{ext}}/E_{\text{grav}}$ on the (x, y) plane. As in the previous case, the external field again contributes substantially to the energy balance of the core, especially near the minimum of the potential well of the cloud. It should be noticed also that what defines the relative importance of W_{ext} is the curvature of the potential field, i.e., the width of the potential, and not only its depth (or height). For instance, the Plummer sphere centered at $x = 12.5$, even though it is more massive, is also more extended, producing a potential well with a larger radius of curvature. This translates into a lower value of W_{ext} at the position of the central region of that sphere, compared to the contribution to W_{ext} of the other Plummer sphere.

One may ask, in general terms, if this potential has places where it can produce disruption or not. To answer this question, in Fig. 8 we show the potential field of the last example (two Plummer spheroids), both in grayscale and in a surface representation, as a function of x and y . First of all, note that the x axis spans up to 20 units, while the y axis spans only 8. Second, note that the plot is symmetric with respect to the axes $x = 0$ and $y = 0$. Third, note also that the dependence on z (not shown here) is the same as the dependence on y .

According to our discussion above, disruption occurs in regions with predominant downwards concavity. In our example (see Fig. 1), the regions that are potentially disruptive are (a) close to $x = 4, y = 0, z = 0$ pc, and (b) regions at large x, y and z . However, as can be seen in Fig. 7, W_{ext} is always compressive ($W_{\text{ext}}/E_{\text{grav}} > 0$ everywhere). The reasons for this are that (a) At large y (or z), the curvature along y is positive (upward concavity). However, the curvature along x is negative, and with a smaller radius of curvature (see

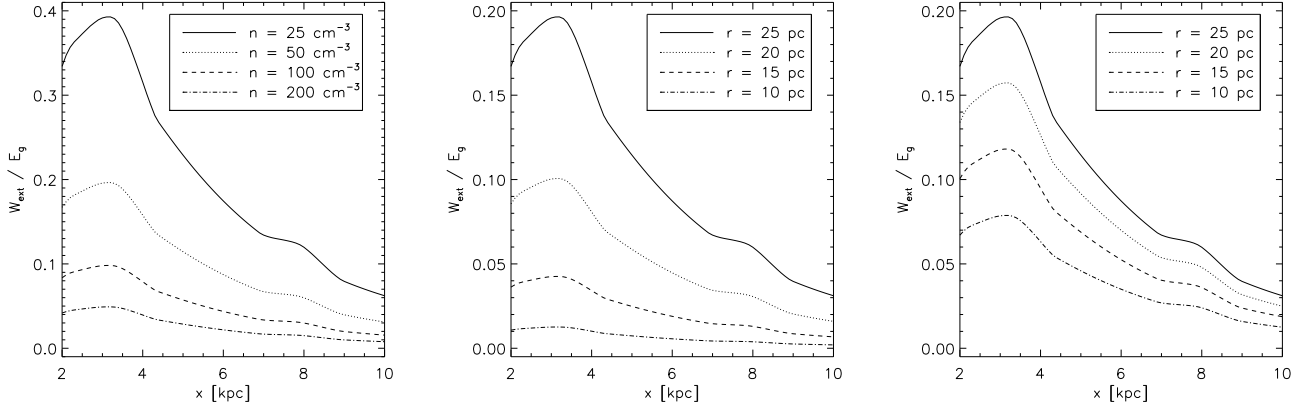


Figure 4. Variation of the ratio $W_{\text{ext}}/E_{\text{grav}}$ for spherical clouds of the same size but different densities (left panel), same mass but different sizes (middle panel), and same column density but different sizes (right panel). Note that $W_{\text{ext}}/E_{\text{grav}} \propto 1/\rho$, for all cases, which implies that $W_{\text{ext}}/E_{\text{grav}} \propto R_{\text{cloud}}^3$ and $W_{\text{ext}}/E_{\text{grav}} \propto R_{\text{cloud}}$ for the cases of constant mass and column density, respectively.

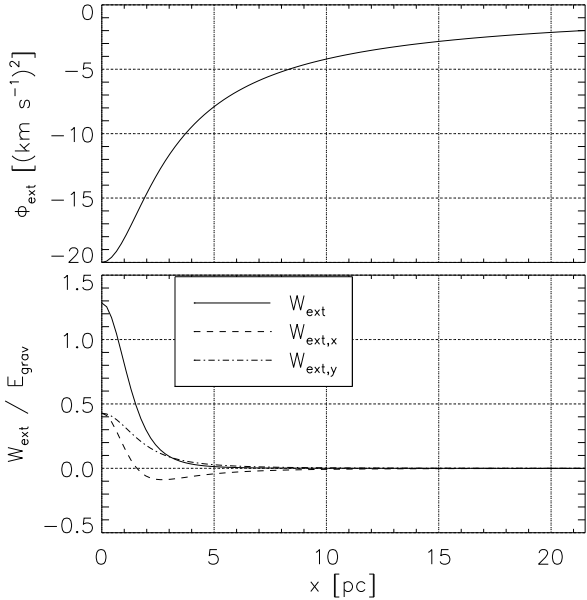


Figure 5. Upper panel: Plummer's potential as a function of the radius, which we take along the x axis. Lower panel: $W_{\text{ext}}/E_{\text{grav}}$ (solid line), $W_{\text{ext},x}/E_{\text{grav}}$ (dashed line) and $W_{\text{ext},y}/E_{\text{grav}}$ (dotted-dashed line) ratios for a $R_{\text{core}} = 0.5$ pc, $n = 3500$ cm $^{-3}$ core embedded in a molecular cloud of $10^4 M_{\odot}$ following a Plummer (1911) potential. Note that the tidal contribution to the energetic content of the core (W_{ext}) are as important as the self-gravitational energy (E_{grav}) of the core.

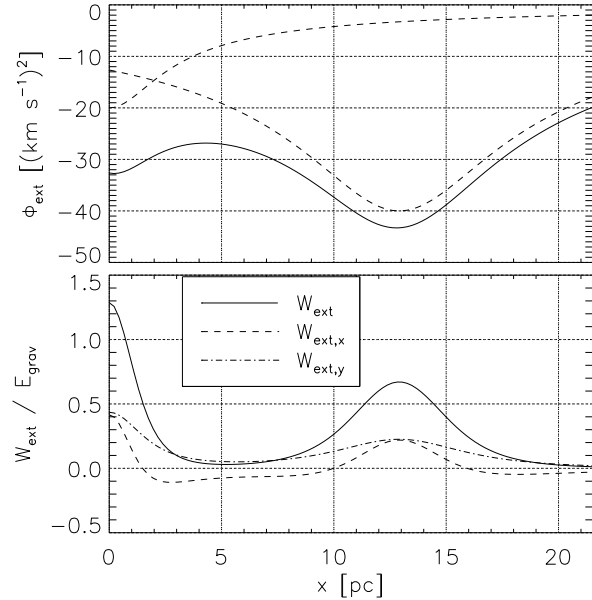


Figure 6. Same as fig. 5, but for a dense core embedded in a gravitational potential given by the superposition of two Plummer spheroids. Dashed lines in the upper panel show the potential of the individual spheroids.

Fig. 8, keeping in mind the different ranges spanned by the axes). Thus, the net effect of $\nabla\Phi_{\text{ext}}$ over the cloud is compressive. (b) The local maximum at $x \sim 4, y = 0, z = 0$ is actually a saddle point, and the concavity along x , although negative, has a larger radius of curvature than the concavity along y , which is positive (again, note that the y axis is more compressed than the x axis). Thus, in both (a) and (b) cases, the positive curvature dominates, producing a positive value for $W_{\text{ext}}/E_{\text{grav}}$. Then, this potential produces compressions everywhere, at least for spherical cores.

Let us now consider an elongated molecular cloud, for which the potential is given by a highly elongated Plummer spheroid that has an aspect ratio of 10 (§3.2). Fig. 9 shows the ratio $W_{\text{ext}}/E_{\text{grav}}$ in this case. The dotted line marks the place where the ratio is equal to zero. We note that the maximum contribution from W_{ext} to the budget is now substantially larger (~ 3.5 times the value of the gravitational energy E_{grav}). This is due to the fact that the density of a filament changes on short scales along the direction perpendicular to its long axis, producing a potential well with small radius of curvature in this direction. Note also that the upper-left region, (above the dotted $W_{\text{ext}}/E_{\text{grav}} = 0$ line), has negative values of the ratio $W_{\text{ext}}/E_{\text{grav}}$, i.e., positive val-

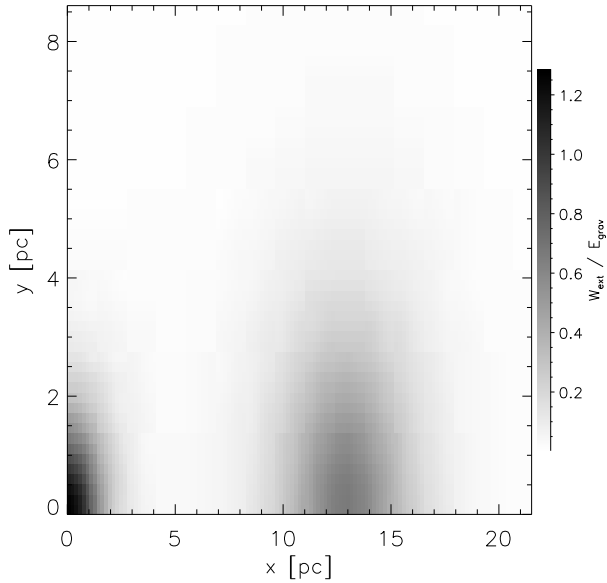


Figure 7. Grayscale two-dimensional version of the lower panel of Fig. 6. Note that the scales in y are expanded by a factor of 2.5. The ratio W_{ext}/E_g has cylindrical symmetry around the x axis.

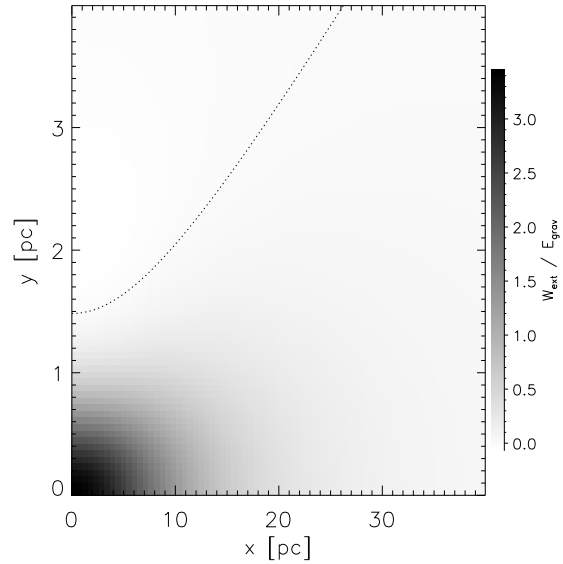


Figure 9. Grayscale of the ratio $W_{\text{ext}}/E_{\text{grav}}$ for a Plummer elongated spheroid, with aspect ratio 10. The dotted line marks the $W_{\text{ext}} = 0$ level (notice that the y axis is expanded by a factor of 10). Elongated structures seem to produce larger values of the ratio $W_{\text{ext}}/E_{\text{grav}}$.

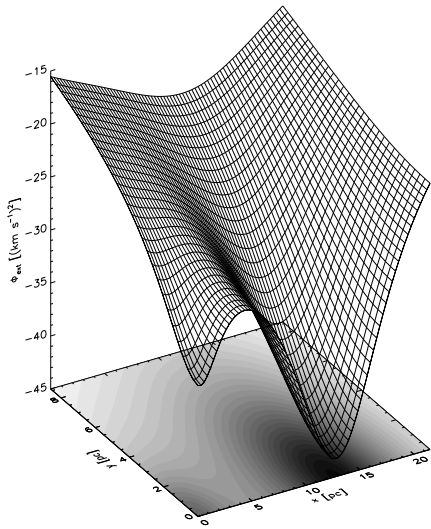


Figure 8. Gravitational potential produced by the superposition of the two Plummer spheroids in the $x - y$ plane, both as a grayscale and surface representation. Both minima occur at $y = 0, z = 0$, while at $x \sim 4$ pc occurs a saddle point. A core located in this point will have strong compression if it is long enough along y , compared to its x -size, but strong disruption if it is long enough in x compared to its y -size (note that the x axis spans up to 20 units, while the y axis spans only 8.)

ues of W_{ext} . Although those values are small, the existence of this region shows that there could be places where an isolated core, in principle, might be disrupted by tidal forces from a larger cloud. However, their small absolute values imply that, if such a core is in energy equipartition between self-gravity and other forms of energy (e.g., magnetic, turbulent, thermal), the tidal disruption will play a negligible role, unless the core is substantially larger than the one modeled here.

In all the cases shown in the present section, the variation of the gravitational potential is soft enough that the external force $\nabla\Phi_{\text{ext}}$ can be considered linear through the size of the core. Thus, as in the case of the GMC embedded in a galactic gravitational field, $W_{\text{ext}}/E_{\text{grav}} \propto 1/\rho$, and our results can be easily translated to cores with different densities. The case of a core within a more realistic parent cloud (e.g., a filamentary GMC from numerical simulations) is deferred to a further contribution.

4.3 General remarks

In summary, for GMCs extended large enough in z within a galactic potential, the external term W_{ext} is negative almost everywhere because the compression along z dominates. However, for clouds confined to the plane of the galaxy (for sizes smaller than 10 pc in z), the galaxy may either compress or disrupt them, depending on the relative orientation between the cloud and the direction of rotation of the galaxy. The spiral arms tend to produce compression, although this also depends on the orientation and the size of the elongated cloud.

In the case of the cores, where we have only considered the effects of the gravitational potential of their parent

cloud, the tidal energy W_{ext} of the structure embedded in a bigger potential can be important close to the local minima, and acts in the same sense than the gravitational energy: by compressing the cloud. We have not found any case in which W_{ext} is positive and comparable to the gravitational energy, suggesting that *the tidal energy of a GMC over its cores helps in their confinement and collapse, but not in their disruption.*

5 DISCUSSION AND CONCLUSIONS

Ranging from GMC sizes (from a few to several tens of parsecs), down to prestellar core sizes (≤ 0.1 pc), molecular clouds and their substructure are often thought to be in virial equilibrium (e.g., McKee & Ostriker 2007, and references therein). This state is inferred from a comparison between their internal (kinetic, thermal, magnetic) and gravitational energies. In previous work, however, we have emphasized the importance of accounting for the role of some additional energy terms that should be considered, but that are usually neglected when the virial theorem is used (see Ballesteros-Paredes & Vázquez-Semadeni 1997; Ballesteros-Paredes et al. 1999a; Ballesteros-Paredes 2006; Dib et al. 2007). In particular, Ballesteros-Paredes (2006) argued that there are at least six assumptions usually made in virial theorem analyses that are frequently not fulfilled in the interstellar medium. In the present work we have focused on the role of the net external potential has on a density structure (a cloud or a core). As a first attempt to evaluate how realistic this assumption is, we have analyzed the contribution of the mass external to the volume of integration to the gravitational term W_{ext} , and compared it to the gravitational energy, in two main cases: a GMC embedded within a spiral galaxy, and a molecular cloud core within its parent molecular cloud.

Although our analysis does not exhaust the possibilities of cloud and core shapes and configurations, the results presented here suggest that by neglecting the influence of the net potential external to a given core, observational estimates can lead to wrong estimations of its actual gravitational content.

We have found that the gravitational field of a Galaxy may have an important influence on the energy budget of GMCs. While the galactic rotation tries to tear apart clouds that are elongated in the radial direction, the field along z tend to compress the clouds. The detailed gravitational content of GMCs depends, thus, on their size, shape, position and orientation within the galaxy. This could be the case, for instance, of Maddalena's cloud, G216-2.5, which exhibits no signs of massive star formation (see, e.g., Megeath et al. 2009, for the current status of star formation going on in G216-2.5), in spite of its having a mass $\sim 6.6 \times 10^5 M_{\odot}$.

The situation for dense cores within simplified potentials for molecular clouds is similar. The gravitational field may tend to disrupt the core in one direction, while compressing it in another. The contribution of W_{ext} depends strongly on the position of the core inside the cloud, and on the details of the gravitational potential of the later. In all the cases shown here, however, this contribution works in the same direction than the self-gravity, i.e., towards compressing the cloud. Moreover, it can be of the order of mag-

nitude or even larger than the gravitational energy, specially in elongated, filamentary clouds. This is due to the fact that filaments can have strong upwards concavity in the direction perpendicular to their main axis.

An interesting result is that tidal disruption tends to be more important than tidal compression for larger objects, while smaller objects tend to suffer larger compressions. The reason for this is that there are no sources of gravitational repulsion, only gravitational attraction. Then, the radii of curvature when the concavity is positive are smaller than when the concavity is negative. This can be pictured by imagining the gravitational field as a tense sheet supporting weights placed on it. On such arrangement, positive (upwards) concavities at the position of the weights have small radii of curvature, while negative (downwards) concavities always extend over larger distances. Thus, for a cloud of moderate size located where the external gravitational field exhibits negative concavity, W_{ext} will be positive, but relatively small with respect to other forms of energy (self-gravity, magnetic, turbulent, etc.). However, if such a cloud is located in a place where the curvature of the external field is positive, its W_{ext} will be important, since the field varies strongly over smaller distances.

As a conclusion, the results shown here suggest that, on large scales, i.e., GMCs within galaxies, the former can be farther from real equipartition, either disrupted or compressed, depending on their shape and orientation within the galaxy. On smaller scales, it seems that it is important to determine observationally the role of the net external potential on local dense cores.

ACKNOWLEDGEMENTS

We thank Paola D'Alessio and Lee Hartmann for a careful reading and useful comments on this manuscript, and to Ian Bonnell, the referee, for an encouraging and useful report. This work was supported by UNAM-PAPIIT grant numbers 110606 and IN119708 to JBP and BP, respectively, and CONACYT grant numbers J50402-F, 50720, and U47366-F to GCG, BP and EVS, respectively. We have made extensive use of the NASA-ADS database. The calculations were performed on the cluster at CRyA-UNAM acquired with grant 36571-E, and on the cluster Platform 4000 (KanBalam) at DGSCA, UNAM.

REFERENCES

- Allen, C., & Santillán, A. 1991, *Revista Mexicana de Astronomía y Astrofísica*, 22, 255
- Ballesteros-Paredes, J. 2006, *MNRAS*, 372, 443
- Ballesteros-Paredes, J., & Hartmann, L. 2007, *Revista Mexicana de Astronomía y Astrofísica*, 43, 123
- Ballesteros-Paredes, J., Hartmann, L., & Vázquez-Semadeni, E. 1999, *ApJ*, 527, 285
- Ballesteros-Paredes, J., & Mac Low, M.-M. 2002, *ApJ*, 570, 734
- Ballesteros-Paredes, J., & Vázquez-Semadeni, E. 1995, *Revista Mexicana de Astronomía y Astrofísica, Conf. Series*, 3, 105

- Ballesteros-Paredes, J., & Vázquez-Semadeni, E. 1997, American xInstitute of Physics Conference Series, 393, 81
- Ballesteros-Paredes, J., Vázquez-Semadeni, E., and Scalo, J. 1999a, *ApJ*, 515, 286–303
- Bertoldi, F., & McKee, C. F. 1992, *ApJ*, 395, 140
- Binney, J., & Tremaine, S. 1987, Princeton, NJ, Princeton University Press, 1987, 747 p.,
- Blitz, L. 1994, *The Cold Universe*, 99
- Briceno, C., Hartmann, L. W., Stauffer, J. R., Gagne, M., Stern, R. A., & Caillaud, J.-P. 1997, *AJ*, 113, 740
- Chandrasekhar, S., & Fermi, E. 1953, *ApJ*, 118, 116
- Dame, T. M., Hartmann, D., & Thaddeus, P. 2001, *ApJ*, 547, 792
- de Jong, T., Boland, W., & Dalgarno, A. 1980, *A&A*, 91, 68
- Dib, S., et al. 2006, *ApJ*, submitted
- Downes, D., Reynaud, D., Solomon, P. M., & Radford, S. J. E. 1996, *ApJ*, 461, 186
- Falgarone, E., Phillips, T. G., & Walker, C. K. 1991, *ApJ*, 378, 186
- Gieles, M., Portegies Zwart, S. F., Baumgardt, H., Athanassoula, E., Lamers, H. J. G. L. M., Sipior, M., & Leenaarts, J. 2006, *MNRAS*, 371, 793
- Goldreich, P., & Kwan, J. 1974, *ApJ*, 189, 441
- Gómez, G. C., Vázquez-Semadeni, E., Shadmehri, M., & Ballesteros-Paredes, J. 2007, *ApJ*, 669, 1042
- Hartmann, L., Ballesteros-Paredes, J., & Bergin, E. A. 2001, *ApJ*, 562, 852
- Heiles, C., & Troland, T. H. 2005, *ApJ*, 624, 773
- Helfer, T. T., Thornley, M. D., Regan, M. W., Wong, T., Sheth, K., Vogel, S. N., Blitz, L., & Bock, D. C.-J. 2003, *ApJS*, 145, 259
- Herbig, G. H. 1978, *Problems of physics and evolution of the universe*, p. 171 - 179, 180 - 188, 171
- Herbig, G. H., Vrba, F. J., & Rydgren, A. E. 1986, *AJ*, 91, 575
- Hunter, J. H., Jr., & Fleck, R. C., Jr. 1982, *ApJ*, 256, 505
- Kegel, W. H. 1989, *A&A*, 225, 517
- Klessen, R. S., Heitsch, F., and Mac Low, M.-M. (2000) *ApJ*, 535, 887–906
- Larson, R. B. 1981, *MNRAS*194, 09–826
- Loinard, L., Dame, T. M., Heyer, M. H., Lequeux, J., & Thaddeus, P. 1999, *A&A*, 351, 1087
- Loinard, L., Dame, T. M., Koper, E., Lequeux, J., Thaddeus, P., & Young, J. S. 1996, *ApJL*, 469, L101
- Maloney, P. 1988, *ApJ*, 334, 761
- McKee, C. F., & Ostriker, E. C. 2007, *ARA&A*, 45, 565
- McKee, C. F. and Zweibel, E. G. 1992, *ApJ*399, 551–562
- Megeath, S.T., Allgaier, E., Young, E., Allen, T., Pipher, J.L., & Wilson, T.L. 2009. *ApJ*, submitted
- Miyamoto, M., & Nagai, R. 1975, *PASJ*, 27, 533
- Myers, P. C., & Goodman, A. A. 1988a, *ApJL*, 326, L27
- Myers, P. C., & Goodman, A. A. 1988b, *ApJ*, 329, 392
- Pichardo, B., Martos, M., Moreno, E., & Espresate, J. 2003, *ApJ*, 582, 230
- Plummer, H. C. 1911, *MNRAS*, 71, 460
- Roberts, W. W., Jr., Huntley, J. M., & van Albada, G. D. 1979, *ApJ*, 233, 67
- Scalo, J. 1990, *ASSL Vol. 162: Physical Processes in Fragmentation and Star Formation*, 151
- Schmidt, M. 1956, *Bull. Astron. Inst. Netherlands*, 13, 15
- Shadmehri, M., Vázquez-Semadeni, E., & Ballesteros-Paredes, J. 2002, *ASP Conf. Ser.* 276: Seeing Through the Dust: The Detection of HI and the Exploration of the ISM in Galaxies, 276, 190
- Shu, F. H., Adams, F. C., & Lizano, S. 1987, *ARA&A*, 25, 23
- Spitzer, L. 1978. *Physical processes in the Interstellar Medium*. New York Wiley-Interscience
- Tilley, D. A., & Pudritz, R. E. 2004, *MNRAS*, 353, 769
- Troland, T. H., & Crutcher, R. M. 2008, *ArXiv e-prints*, 802, arXiv:0802.2253
- Vázquez-Semadeni, E., Ballesteros-Paredes, J., & Rodríguez, L. F. 1997, *ApJ*, 474, 292
- Vázquez-Semadeni, E., Gómez, G. C., Jappsen, A. K., Ballesteros-Paredes, J., González, R. F., & Klessen, R. S. 2007, *ApJ*, 657, 870
- Vázquez-Semadeni, E., González, R.F., Ballesteros-Paredes, J., Gazol, A., & Kim, J. 2008. *MNRAS*, submitted
- Wilson, R. W., Jefferts, K. B., & Penzias, A. A. 1970, *ApJL*, 161, L43
- Young, J. S., & Scoville, N. Z. 1991, *ARA&A*, 29, 581
- Zuckerman, B., & Evans, N. J., II 1974, *ApJL*, 192, L149